Effects of Zinc Oxide Nanoparticles on the Physical Properties of Polyacrylonitrile

Dong Wook Chae, Byoung Chul Kim

Division of Applied Chemical Engineering, Hanyang University, Haengdang, Seongdong, Seoul 133–791 South Korea

Received 21 February 2005; accepted 29 June 2005
DOI 10.1002/app.22533
Published online in Wiley InterScience (www.interscience.wiley.com).

ABSTRACT: Polyacrylonitrile (PAN)/zinc oxide (ZnO) nanocomposites were prepared by solution mixing in dimethylacetamide, followed by film casting, and their physical properties were investigated. The heating scan of differential scanning calorimetry displayed only a single crystallization peak (T_c) without a melting peak, regardless of the presence of ZnO. The incorporation of ZnO nanoparticles decreased T_c by 13°C, and increased the heat of crystallization by 18%. Further, it greatly improved the thermal stability of PAN, even at the ZnO content as low as 0.1 wt %. The nanocomposites showed the UV transmittance peak at 365 nm, whose intensity was increased as ZnO content was increased. The presence of ZnO did not produce new peak nor shift the peaks with respect to PAN in wide angle X-ray diffraction pattern. Introduction of a small amount of ZnO nanoparticles did not have notable effect on the tensile properties. However, 5 wt % loading of the nanoparticles increased the tensile modulus of PAN by 14.5% and decreased elongation at break dramatically. PAN nanocomposites with 5 wt % ZnO did not show any plateau region in stress–strain curve.
 J Appl Polym Sci 99: 1854–1858, 2006

Key words: nanocomposites; polyacrylonitrile; zinc oxide; physical properties

INTRODUCTION

Because of extremely large specific surface area, incorporation of inorganic and metal nanoparticles into organic polymers usually exerts unique physical and chemical properties, which cannot be shared by conventional polymer composites. Some advantages of nanocomposites include high stiffness, flame retardency, higher heat distortion temperature and enhanced thermal stability, lower gas and fluid permeability, and chemical resistance without sacrificing optical properties.[1–6] Further, these improved properties are usually obtained at much lower content than micron particles.[7] Thus, modification of organic polymers with inorganic nanoparticles draws much attention because the nanocomposites are expected to find new commercial applications.

Polyacrylonitrile (PAN) is mainly used to produce synthetic fibers. PAN is highly polar with strong interchain interactions through nitrile groups and cannot be melt processed because it decomposes before it softens sufficiently for melt fabrication. Hence, PAN fibers are spun from solution in highly polar solvent such as dimethylformaide, dimethylacetamid, or dimethylsulphoxide. Zinc oxide (ZnO) has been widely used in UV protection, protection from microorganism, photocatalysis, field emission displays, varistors, functional devices, and thermoelectric materials.[8,9] In addition, dispersed metal oxides play a role of stabilizing agent to polymers through direct interaction with macromolecules and supermolecular structure.[10] As a rule, the extent of property enhancement depends on factors such as nanoparticle size, size distribution, aspect ratio, degree of dispersion and orientation in the matrix, and the adhesion at the filler–matrix interface.[11–15]

Extensive work has been done in polymer–clay nanocomposites and its application made commercial success in nylon 6.[16–18] This can pave the way to develop various nanoparticle-filled polymer composites such as metal oxides, mineral powders, and carbon. In addition, diverse methods have been adopted to disperse homogeneous nanoparticles into polymer. Typically, the nanocomposites are obtained by either *in-situ* polymerization or the direct melt compounding.[17–23] A majority of current researches have focused on the former, but its application is limited. The problem most frequently encountered with melt mixing is particle agglomeration. This may be overcome by solution mixing. In this study, PAN/ZnO nanocomposites were prepared by solution mixing, followed by film casting, and the effect of ZnO on the morphological and physical properties of PAN was investigated by microscopic, spectroscopic, thermal, and mechanical analysis.

EXPERIMENTAL

Materials

ZnO nanopowder (average size 87 nm, standard deviation = 42) was purchased from Aldrich. PAN (M_n

Correspondence to: B. C. Kim (bckim@hanyang.ac.kr).

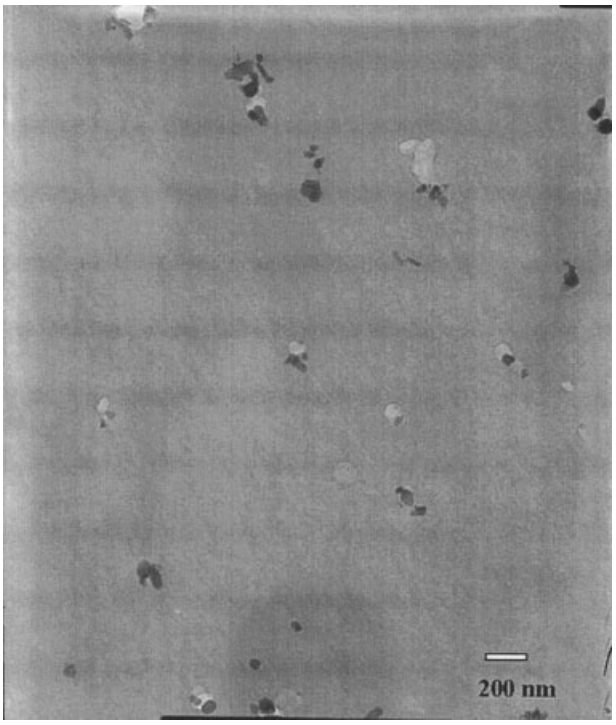

Figure 1 TEM images of PAN nanocomposites with 5 wt % ZnO.

= 86,200) was a commercial product purchased from Aldrich. *N*,*N*-dimethylacetamide (DMAc; Kento Chemical Co., Japan) was selected as a solvent of the polymers because it also showed a good dispersion of ZnO nanoparticles. ZnO was first dispersed in DMAc. To break apart the agglomerate of ZnO, an ultrasonic vibration was applied for 10 min. PAN was then dissolved in the solutions at 70°C with vigorous stirring. Final concentration of PAN in DMAc was 10 wt %. ZnO contents (*X*) were 0.1, 1, 2, and 5 wt % based on the polymer matrix, and they were coded PAN-*X*. To get a nanocomposite film, the PAN/ZnO solutions were cast at 80°C for 4 days. For complete evaporation, the solvent-cast film was vacuum-dried at 100°C for 5 days.

Measurement of physical properties

Transmission electron microscopy (TEM) experiments were carried out with a JEOL JEM-2000FXII applying an acceleration voltage of 200 kV. The specimen was prepared using an ultramicrotome. Thin sections of about 100 nm thickness were cut with a diamond knife. The morphology of PAN/ZnO nanocomposites was examined with a field emission scanning electron microscope (FESEM; JEOL, JSM-6330F) whose surface was coated with gold under vacuum.

UV spectra of the nanocomposite film, with a thickness of 5 μm, were recorded on a Perkin–Elmer Lambda 25 UV spectrometer.

Wide angle X-ray diffraction (WAXD) experiments were carried out by Rigaku Denki (D/MAX-2000) with Nickel-filtered Cu Kα radiation of 40 kV and 100 mA. Scanning was carried out on the equator in the 2θ range from 5° to 80° at a scan speed of 5°/min.

Differential scanning calorimetry (DSC) experiments were carried out on a DSC 2010 (TA Instruments, Dupont). Heating scans were performed at a rate of 10°C/min in a nitrogen atmosphere. Thermal gravimetric analysis (TGA) was carried out using SDT 2960 (TA Instruments, Japan). Samples were heated to 1000°C at a heating rate of 10°C/min in a nitrogen atmosphere.

The mechanical properties were measured by using dog-bone-shaped specimens (ASTM D 638 Type V) on an Instron tensile tester model 4465 at room temperature. The gauge length and crosshead speed were 25 and 5 mm/min, respectively. The mean values of 10 measurements were taken as the data.

RESULTS AND DISCUSSION

Figure 1 shows the TEM images of PAN nanocomposites with 5 wt % ZnO. ZnO nanoparticles are well dispersed in PAN matrix without forming large clusters. Hydrophilic features of ZnO produce a uniform dispersion in the polar solvent, DMAc. That is, a strong interaction between solvent and nanoparticle plays a crucial role in breaking the large agglomerate present in dry state. In addition, it prevents the reagglomeration of the nanoparticles, which may occur in film casting processing. The FESEM images of PAN nanocomposites with 1 wt % ZnO are shown in Figure 2. The size of ZnO particles embedded in PAN is similar to that of primary particle. The FESEM images in film state also show that the nanoparticles are homogeneously dispersed without large agglomerate.

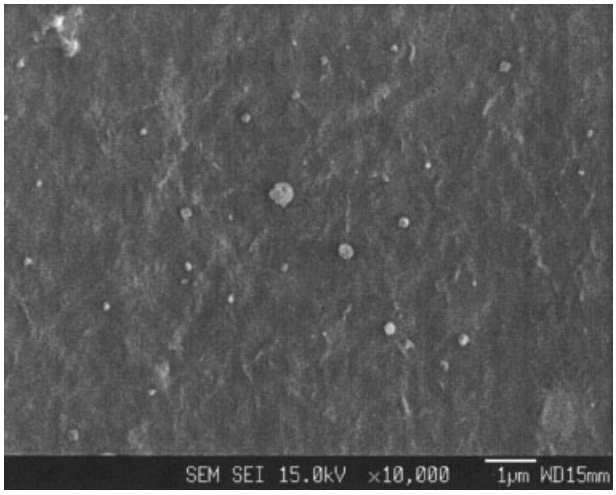

Figure 2 FESEM images of PAN nanocomposites with 1 wt % ZnO.

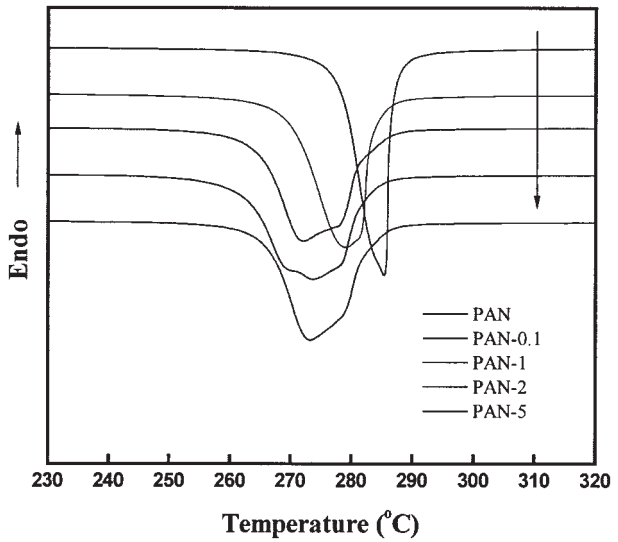

Figure 3 DSC heating scan thermograms of PAN and PAN/ZnO nanocomposites.

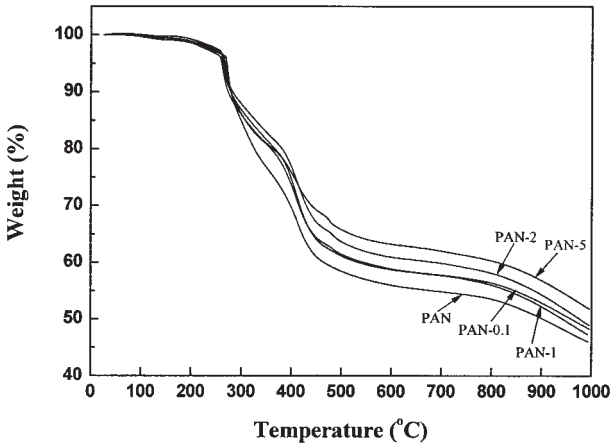

Figure 4 TGA thermograms of PAN and PAN/ZnO nanocomposites.

The heating scan thermograms of DSC of PAN and PAN/ZnO nanocomposites are shown in Figure 3 and the results are summarized in Table I. They present a single crystallization peak (T_c) without a melting peak. The incorporation of ZnO nanoparticles decreases T_c from 285.4 to 272.1°C, and increases the heat of crystallization (ΔH_c) from 497.9 to 589.7 J/g. In particular, even at the low content 0.1 wt %, T_c is decreased by 6.3°C and ΔH_c is increased by 11.5%. This suggests that ZnO nanoparticles accelerate crystallization through heterogeneous nucleation and increase the degree of crystallinity. In addition, the width of crystalline peak of the nanocomposites becomes broader. The interfacial region in nanoparticle-filled polymers may be described as a polymer layer to include a region of immobile polymer due to a polymer–particle interaction and narrow space surrounded by the dispersed nanoparticles. Thus, this restricted segmental motion near the organic–inorganic interfaces accounts for the broadening in T_c.

Figure 4 shows the TGA curves of pure PAN and PAN/ZnO nanocomposites. The thermal stability of the nanocomposites is greatly improved in the high temperature range, even at the content of ZnO as low as 0.1 wt %. This suggests that adhesion between polymer and inorganic surface makes contribution to enhancement of thermal stability. The samples show the decomposition temperature measured as the temperature required for 10% degradation at 278°C, little dependent upon the presence of the nanoparticles. However, with proceeding degradation, greater resistance to degradation is observed at high ZnO content. The improvement in the thermal stability of the nanocomposites should be ascribed to heat shielding effects of ZnO nanoparticles. Especially, PAN-5 shows much higher degradation temperature required for 40% degradation by 347°C in comparison with pure PAN. This implies that the role of nanoparticles on the degradation is efficient under unfavorable condition.

TABLE I
Crystallization Behavior During Heating Scan for PAN and PAN/ZnO Nanocomposites

	T_c (°C)	ΔH_c (J/g)
PAN	285.4	497.9
PAN-0.1	279.1	555.2
PAN-1	272.1	562.1
PAN-2	273.7	589.7
PAN-5	273.2	553.7

The effects of ZnO nanoparticles on the UV–visible transmittance of PAN are demonstrated in Figure 5. While PAN-0.1 shows almost the same UV transmittance as pure PAN, the nanocomposites with ZnO more than 1 wt % show the transmittance peak at 365 nm whose intensity is increased with ZnO content. Thus, application of ZnO-filled system is of great help to screening the harmful UVA radiation (315–400 nm). In addition, the difference of transmittance becomes negligible at ZnO content more than 2 wt %.

The WAXD patterns of pure PAN and PAN/ZnO nanocomposites are shown in Figure 6. All the samples show a sharp crystalline peak (17.3°) and a broad noncrystalline peak (20°–30°). PAN is unusual in that even atactic molecules can crystallize. The characteristic peak at 17.3°corresponds to orthorhombic PAN (110) reflection.[24] In addition, the diffraction peaks at 2θ = 31.9°, 33.3°, 36.4°, 47.7°, 56.7°, 63.0°, 66.5°, 68.1°, 70.0°, and 77.1°, which become notable with increasing ZnO content, are assigned to the crystallographic planes of ZnO (100), (002), (101), (102), (110), (103), (200), (112), (201), and (202), respectively. However, the incorporation of ZnO nanoparticles does not pro-

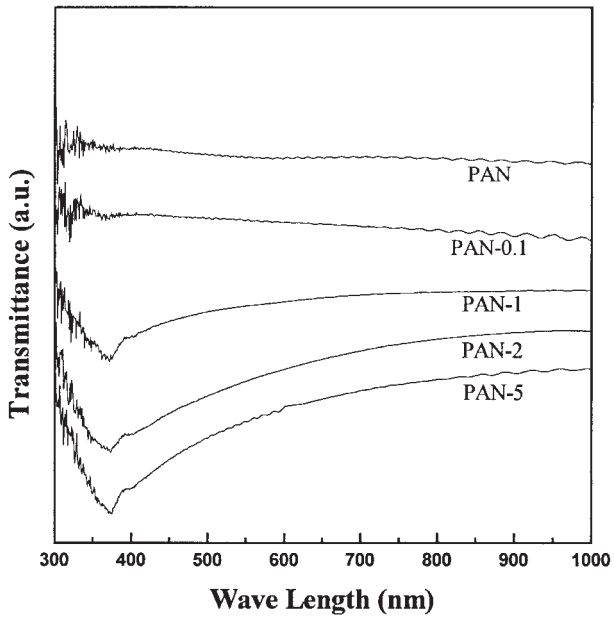

Figure 5 UV spectra of PAN and PAN/ZnO nanocomposites.

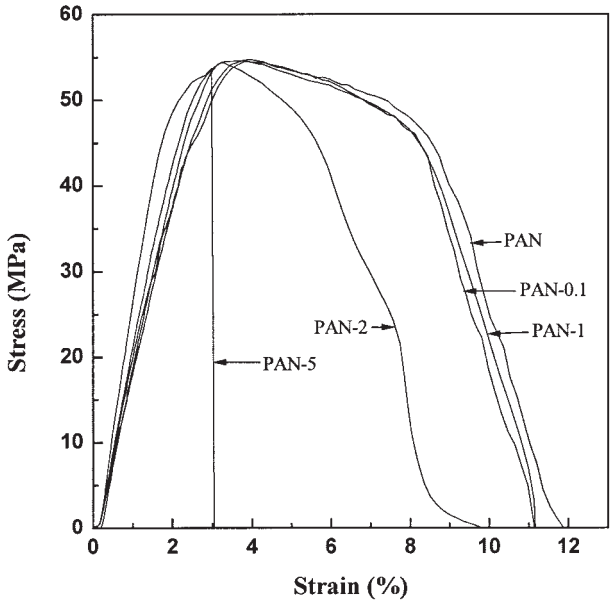

Figure 7 Strain–stress curve of PAN and PAN/ZnO nanocomposites.

duce any new peak and peak shift with respect to pure PAN. This reveals that the PAN/ZnO nanocomposites exhibit a two-phase structure consisting of polymer and nanoparticle.[25]

As shown in Figure 7, the introduction of ZnO nanoparticles modifies the shape of stress–strain (SS) curve. In the presence of ZnO nanoparticle more than 2 wt %, the range of likely plateau region, where the stress decrease slowly with strain, becomes short. In particular, PAN-5 shows no plateau region, a typical SS curve of brittle material. PAN nanocomposites with 5 wt % ZnO show slightly decreased tensile strength by 4%, as given in Table II. At high ZnO content, dewetting between filler and matrix phases under extension reduces the surface area in contact with the nanoparticles and also becomes the site of stress concentration, giving rise to a microcrack initiator due to poor stress transfer at the interface. According to Griffith's theory, if a large flaw exists within an area of stress concentration, the tensile strength is reduced.[26] ZnO nanoparticles embedded in the PAN matrix increase the tensile modulus of the polymer, which is more notable at higher ZnO content. However, the elongation at break is notably decreased at high ZnO content. The fracture resistance is decreased progressively with increasing nanoparticle content because of reduced amount of polymer matrix, which absorbs propagation energy of fracture.[27] In addition, the nanoparticles may form agglomerates at high content, resulting in dramatic reduction in toughness.

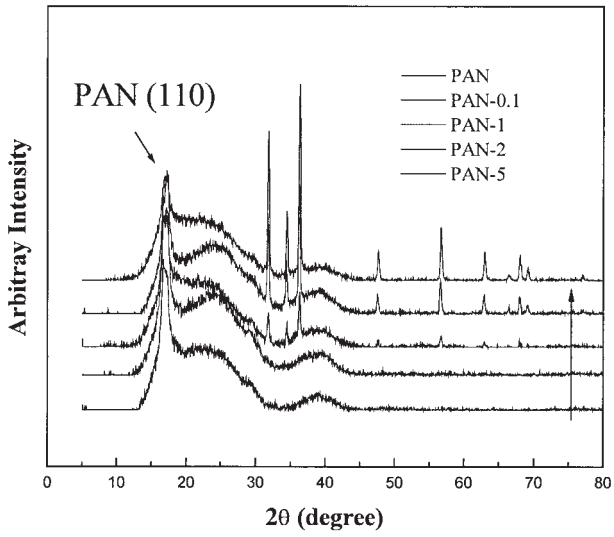

Figure 6 WAXD profiles of PAN and PAN/ZnO nanocomposites.

Figure 8 exhibits the FESEM images of tensile fractured surface of PAN and PAN/ZnO nanocomposites. Pure PAN displays wedge-shaped surface having somewhat sharp tip. However, ZnO-filled systems show that the fracture surface are composed of large bundles in which the polymer chain may be stuck to a particle surface, which may result from the interaction between polymer and nanoparticle. That is, good adsorption of polymer chains to the nanoparticles makes the samples fractured in a state of a large bundle containing immobile polymer chain. The region of immobile polymer is increased with loading level having a significant effect on the properties of the composites. In addition, the pull-out of the ZnO in PAN matrix is not observed in the fractured surface, indicating good adhesion between ZnO nanoparticle and PAN matrix.

TABLE II
Effects of ZnO Nanoparticles on the Tensile Properties of PAN

Tensile properties	Sample				
	PAN	PAN-0.1	PAN-1	PAN-2	PAN-5
Tensile strength (MPa)	55.3	55.9	56.6	56.1	53.2
Tensile modulus (MPa)	2370	2386	2443	2513	2714
Elongation at break (%)	11.64	10.64	10.61	10.05	3.85
Toughness (MPa)	2.97	2.89	2.90	2.63	0.88

CONCLUSIONS

Solution mixing made it possible homogeneous dispersion of ZnO nanoparticles in the PAN matrix. This improved the thermal stability of PAN because of the barrier role of ZnO to the heat. In addition, the ZnO nanoparticles decreased the maximum crystallization temperature of PAN and increased the width of crystallization peak, suggesting heterogeneous nucleation and hindered mobility of polymer chains. The introduction of ZnO nanoparticles increased the tensile modulus but reduced the toughness of PAN. So, the nanoparticle content should be determined in service purpose because the improved modulus is obtained at the cost of a decrease in strength and elongation.

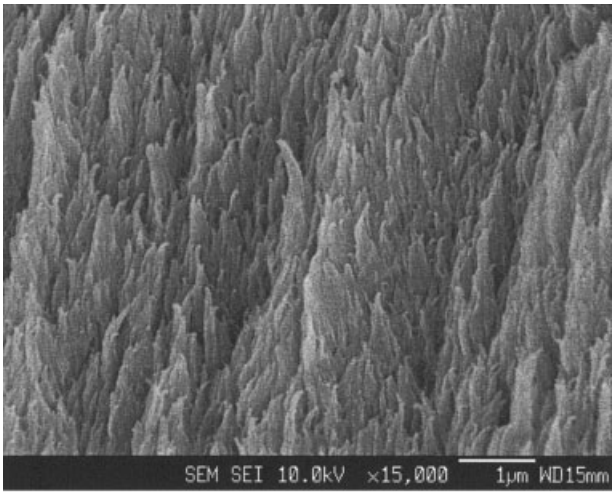

(a)

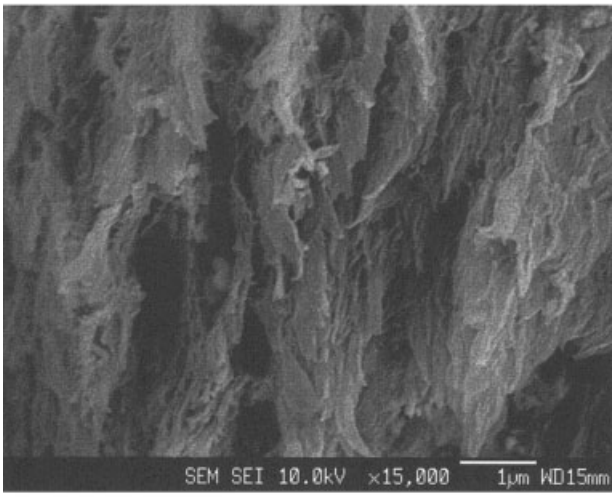

(b)

Figure 8 FESEM images of tensile fractured surface of (a) PAN and (b) PAN-5.

References

1. Grocela, T. A.; Nauman, E. B. Polymer 1993, 34, 2315.
2. Gleiter, H. Adv Mater 1992, 4, 474.
3. Saujanya, C.; Radhakrishnan, S. Polymer 2001, 42, 6723.
4. Yano, K.; Usuki, A.; Yurauchi, T.; Kamigaito, O. J Polym Sci Part A: Polym Chem 1993, 31, 2493.
5. Smoug D. Mod Plast 1998, 2, 28.
6. Min, Z. R.; Ming, Z. Q.; Yong, X. Z.; Han, Z. M.; Walter, R.; Friendrich, K. Polymer 2001, 42, 167.
7. Zilg, C.; Reichert, P.; Dietsche, F.; Engelhardt, T.; Mülhaupt, R. Kunststoffe 1998, 88, 1812.
8. Wang, Z.; Li, H. J. Appl Phys A 2002, 74, 201.
9. Tsuzuki, T.; McCormick, P. G. Scripta Mater 2001, 44, 1731.
10. Gordienko, V. P.; Dmitriev, Y. A. Polym Degrad Stab 1996, 53, 79.
11. Embs, F. W.; Thomas, E. L.; Wung, C. J.; Prasad, P. N. Polymer 1993, 34, 4607.
12. Calvert, P.; Burdon, J. Polym Mater Sci Eng 1994, 70, 224.
13. Karokawa, Y.; Yasuda, H. J Mater Sci Lett 1966, 15, 1481.
14. Wang, Y.; Huang, J. S. J Appl Polym Sci 1996, 60, 1779.
15. Ettlinger, M.; Ladwig, T.; Weise, A. Progr Org Coating 2000, 40, 31.
16. Kojima, Y.; Usuki, A.; Kawasumi, M.; Okada, A.; Kurauchi, T.; Kamigaito, O.; Kaji, K. J Polym Sci Part B: Polym Phys 1995, 33, 1039.
17. Qi, R.; Jin, X.; Nie, J.; Yu, W.; Zhou C. J Appl Polym Sci 2005, 97, 201.
18. Xiao, W.; Yu, H.; Han, K.; Yu, M. J Appl Polym Sci 2005, 96, 2247.
19. Yang, F.; Ou, Y.; Yu, Z. J Appl Polym Sci 1998, 69, 355.
20. Kojima, Y.; Usuki, A.; Kawasumi, M.; Okada, A.; Kurauchi, T.; Kamigaito, O. J Appl Polym Sci 1993, 49, 1259.
21. Lee, D. C.; Jang, L. W. J Appl Polym Sci 1998, 68, 1997.
22. Fornes, T. D.; Yoon, P. J.; Keskkula, H.; Paul, D. R. Polymer 2001, 42, 9929.
23. Liu, L.; Qi, Z.; Zhu, X. J Appl Polym Sci 1999, 71, 1133.
24. Sawai, D.; Miyamoto, M.; Kanamoto, T.; Ito, M. J Polym Sci Part B: Polym Phys 2000, 38, 2571.
25. Zhang, Z.; Zhang, L.; Wang, S.; Chen, W.; Lei, Y. Polymer 2001, 42, 8315.
26. Griffith, A. A. Philos Trans R Soc London Ser A 1920, 221, 163.
27. Thio, Y. S.; Argon, A. S.; Cohen, R. E.; Weinberg, M. Polymer 2002, 43, 3661.